Structural Engineering and Mechanics, *Vol. 59, No. 4 (2016) 703-718*
DOI: http://dx.doi.org/10.12989/sem.2016.59.4.703

Assessment of load carrying capacity and fatigue life expectancy of a monumental Masonry Arch Bridge by field load testing: a case study of veresk

Shervan Ataei[a], Mosab Tajalli[b] and Amin Miri*

School of Railway Engineering, Iran University of Science and Technology, Narmak, Tehran, Iran

(Received November 4, 2015, Revised May 15, 2016, Accepted June 23, 2016)

Abstract. Masonry arch bridges present a large segment of Iranian railway bridge stock. The ever increasing trend in traffic requires constant health monitoring of such structures to determine their load carrying capacity and life expectancy. In this respect, the performance of one of the oldest masonry arch bridges of Iranian railway network is assessed through field tests. Having a total of 11 sensors mounted on the bridge, dynamic tests are carried out on the bridge to study the response of bridge to test train, which is consist of two 6-axle locomotives and two 4-axle freight wagons. Finite element model of the bridge is developed and calibrated by comparing experimental and analytical mid-span deflection, and verified by comparing experimental and analytical natural frequencies. Analytical model is then used to assess the possibility of increasing the allowable axle load of the bridge to 25 tons. Fatigue life expectancy of the bridge is also assessed in permissible limit state. Results of F.E. model suggest an adequacy factor of 3.57 for an axle load of 25 tons. Remaining fatigue life of Veresk is also calculated and shown that a 0.2% decrease will be experienced, if the axle load is increased from 20 tons to 25 tons.

Keywords: Masonry Arch Bridge; train load testing; finite element model calibration; load carrying capacity; fatigue life estimation

1. Introduction

Aiming at increasing the throughput of the network, railway administrators seek out new solutions such as increasing the axle load or operational speed of trains to allow more trains in the network. One major obstacle in doing so is the limited capacity of existing structures in the network such as bridges. In this regard, evaluating the performance of such structures subjected to different loading schemes and operational speeds seem to be the prerequisite of increasing the axle load.

Iranian railway organization has started a project of increasing the axle load of its railway network from the current 20 tons to 25 tons. One major problem is the existence of old masonry bridges in the network such as Veresk bridge, which is a plain concrete masonry arch bridge built

*Corresponding author, Master of Science, E-mail: amin.miri.iust@gmail.com
[a]Ph.D., E-mail: ataei@iust.ac.ir
[b]Ph.D. Student, E-mail: mosabtajalli@gmail.com

http://www.techno-press.org/?journal=sem&subpage=8 ISSN: 1225-4568 (Print), 1598-6217 (Online)

more than 80 years ago. The problem with evaluating the performance of Veresk is the complexity of Masonry Bridge's behavior, which has been of great debate during recent years.

There are a number of methods proposed for the evaluation of load carrying capacity of masonry bridges, including empirical methods such as MEXE (1997), yield design based methods (Havey 1988, Clemente *et al.* 1995), fiber beam elements method (Felice 2009), and those employing a scaled model of the bridge (Prentice and Ponniah 1994, Cancelliere *et al.* 2010).

Recently a number of studies have successfully assessed the load carrying capacity of masonry bridges by 2D and 3D finite elements models (Bayraktar *et al.* 2010, Chandra *et al.* 2013, Marefat *et al.* 2004, Helmerich 2010, Oliveira *et al.* 2010, Caglayan *et al.* 2012, Brencich and Sabia 2007, Ataei *et al.* 2016). Caligyan *et al*. (2012) have conducted static and dynamic tests on a concrete arch bridge and used test results to calibrate the 3D model of the bridge. Marefat *et al*. (2004) have conducted static tests on a decommissioned masonry railway arch bridge. They concluded that despite initiation of cracks on the bridge structure, the bridge sustained loads much higher than the service load. Brencich and Sabia (2007) have conducted dynamic tests on a bridge with 18 spans of 10 meters. They used the test results to determine mode shapes and natural frequencies of the bridge and concluded that multiple spots on the bridge have to be instrumented in order to determine the mode shapes of the bridge by dynamic tests.

Fatigue life expectancy is also a vital factor to be considered in feasibility study of increasing the axle load of old bridges. Casas (2009) proposed a probabilistic model to study the fatigue life of brick masonry under compressive stress. Casas concluded that the fatigue life of masonry is related to both maximum and minimum stresses applied to it. Melbourne *et al.* (2004) have conducted laboratorial tests on multi-ring masonry arches and assessed their load capacity, along with endurance limit. Results suggested that arch's cyclic capacity and endurance limits are about 60% less than arch's static capacity. It is also concluded that ring separation mechanism occurs prior to 4-hinge mechanism in multi-ring arches. In a recent study by Newhook *et al*. (2013), reliability concept and structural health monitoring are combined to develop a model for fatigue cracking issues of a concrete bridge deck. The model consists of 5 components: a vehicle load model, a fatigue damage accumulation model, a residual strength model, a reliability model and a structural health monitoring decision model. The model is then used to develop a decision threshold for the oldest concrete bridge deck in service.

This paper aims at presenting the result of field tests carried out on one of the oldest masonry arch bridges of Iranian railway network to determine whether it is possible to increase the currently 20 tons axle load applied to the bridge to 25 tons. For this purpose, the bridge is loaded with the maximum allowable axle load of the bridge (which is 20 tons) and its response recorded by different sensors. Although the difference between applied axle load and intended future axle load is high, it is not possible to apply higher axle loads on the bridge due to safety concerns.

A 3D finite element model is developed in a commercial finite element software. The model is calibrated by comparing experimental and analytical mid-span deflections, and verified by comparing experimental and analytical natural frequencies. The numerical model is then used to assess the possibility of increasing the allowable axle load of the bridge. It is also used to determine the ultimate load carrying capacity of the bridge and its remaining fatigue life. Methodology research is schematically presented in Fig. 1.

2. Bridge characteristics

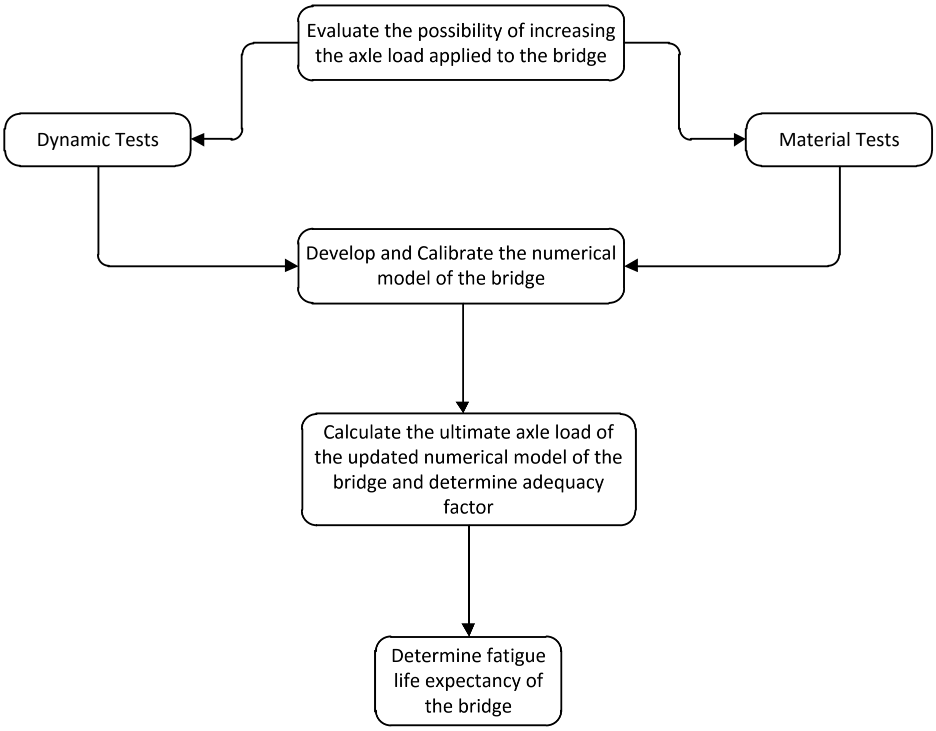

Fig. 1 Research methodology

Fig. 2 Veresk during construction in 1935

Veresk is a plain concrete arch bridge built in 1936 in the northern part of Iranian railway network. It is also registered as a national heritage site due to its stylish architecture. The concrete

Fig. 3 Eastern view of Veresk

Fig. 4 Core taken from bridge pier to be tested for concrete characteristics

structure beneath the bridge was used as a temporary framework during the construction of the bridge, as depicted in Fig. 2. The bridge, which is built of concrete blocks, consists of a central arch of 66 meters, which is one of the longest in Iranian railway network, and 8 piers that rest on rock bed and the arch itself, as shown in Fig. 3. Veresk has a total length of 100 meter, and has a height of 110 meters from the bottom of the valley. The main arch's width varies between 4.9 to 6 meters, with a steep gradient of 0.028%. Main arc's thickness varies from 2.8 meter in the restraints to 1.6 meter in the middle of the span.

The bridge has been visually inspected and no observable cracks were spotted in the structure. In order to have the characteristics of the material used in building Veresk, a series of tests have been conducted. Cores from 7 spots of the bridge are taken to a lab and tested to determine the characteristics of concrete, as shown in Fig. 4. Table 1 presents the material characteristics that are used in the numerical model.

Since mortar is used to fill up the gap between concrete blocks, elasticity modules of masonry needs to be calculated and used in the model. To do so, the following equation is used (SB 4.7)

$$E = \frac{E_m E_b (t_m + t_b)}{(E_m t_b + E_b t_m)} \tag{1}$$

Table 1 Material characteristics used in the model

Material	Compressive Strength (MPa)	Elasticity Modules (GPa)	Poisson Ration	Weight per unit of volume (Kg/m^3)
Arch and Pier Concrete	28	25.0	0.167	2400
Filler Concrete	15	18.3	0.167	2400
Ballast	-	0.3	0.200	1900

In which:

Em - modulus of elasticity of the joint,

Eb - modulus of elasticity of the stone/brick unit,

tm - thickness of the mortar joint,

tb - thickness of stone/brick unit

Concrete blocks have a thickness of 25 cm, and filler concrete has a thickness of 2 cm. Using Table 1 and Eq. (1), a masonry elasticity module of 23.5 GPa is calculated. Compressive strength of masonry could also be determined by the following equation (UIC 778-3 2006)

$$f_k = 0.5 f_b^{0.65} f_m^{0.25} \tag{2}$$

In which:

F_k=*compressive strength of masonry,*

F_b=*compressive strength of concrete,*

F_m=*compressive strength of mortar*.

Using Table 1 and Eq. (2), compressive strength of masonry is 7.3 MPa.

3. Test Instrumentation and procedures

A calculated assessment presumes that together with the geometry, foundations and load, all essential material properties and their status are known or can be estimated and that the load transfer can be described realistically in mathematical terms (UIC 778-3). In reality, however, it is fairly difficult to determine the exact material properties of the whole material in building masonry bridges. There are sometimes ambiguities in the structure of such bridges as well. In such cases, field tests are one useful way of determining the overall behavior of the bridge, due to applying predefined loading schemes.

The aim of field tests is to determine the response of Veresk to the passage of the test train. For this purpose, vertical deflection of middle and quarter span of the main arch, along with vibrations at 5 spots on the arch are selected to be monitored. Since Veresk is of heritage value, all sensors are mounted on plastic frames glued to the bridge surface, and later taken off.

Deflection of arch is supposed to be recorded with a frequency and accuracy of at least 10 Hz and 100 μm, respectively. Ordinary displacement recording sensors require a reference point on which the deflection meter is fixed, and any displacement relative to the fix point is recorded. The only reference point in the vicinity of Veresk is the concrete structure 20 meters below the main arch, which makes it practically impossible to install ordinary deflection recording sensors on the bridge. For this reason, another type of deflection recording sensor called 'Deflected Cantilever Displacement Transducer', or simply put 'DCDT', is used. DCDTs come with a cable that is fixed

Fig. 5 Fixing DCDT's cable to the concrete structure beneath Veresk

Fig. 6 LVDT sensor mounted on sleeper to monitor train movement

to a reference point, for which the concrete structure beneath the bridge is used (Fig. 5). This sensor is capable of recording the displacement in a range of 25 mm with an accuracy of 10 μm. Since the concrete structure is inaccessible by foot, bridge monitoring machine is employed to reach the concrete structure beneath Veresk, as shown in Fig. 5.

To determine the exact speed and location of test train on the bridge, a series of LVDT sensors and strain gauges are mounted on the rail, as shown in Figs. 6 and 7. Furthermore, bridge vibrations under moving load are recorded by 5 accelerometers. Overall, 12 sensors are mounted on Veresk as depicted in Fig. 8. Throughout the tests, data is recorded with a frequency of 1 KHz.

Fig. 7 Strain gauge mounted on rail heel to monitor train position during the tests

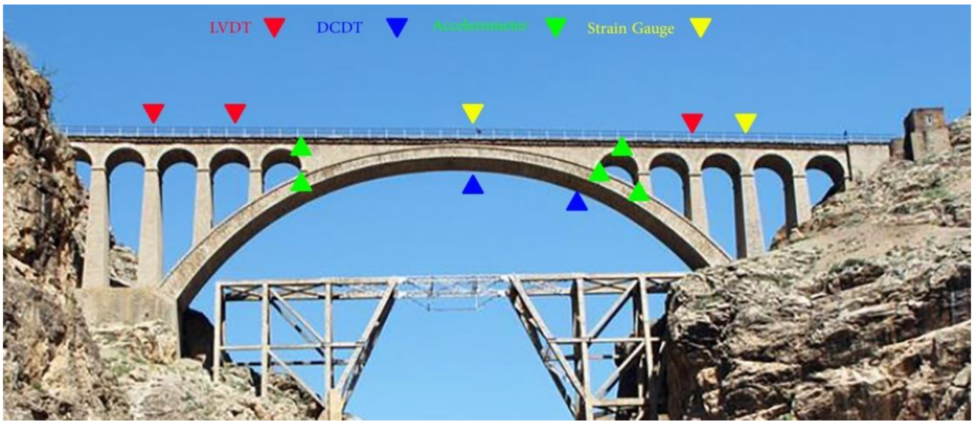

Fig. 8 Instrumentation of Veresk

Two 6-axle locomotives and two 4-axle freight wagons are used to form the test train. Axle spacing and loads are presented in Fig. 9, schematically. A total of 28 dynamic tests are carried out on the bridge, in which test train is passed through the test site in both directions with speeds of 3.5, 35, 40, 45, 50, 55, and 60 km/h.

4. Test results

Fig. 10 presents the response of the bridge in terms of vertical deflection of middle and quarter span of main arch as test train passes over Veresk with a speed of 50 Km/h. A bump is observable in the vertical deflection signature of middle span, which is due to the passing of higher axle load of locomotive.

(a)

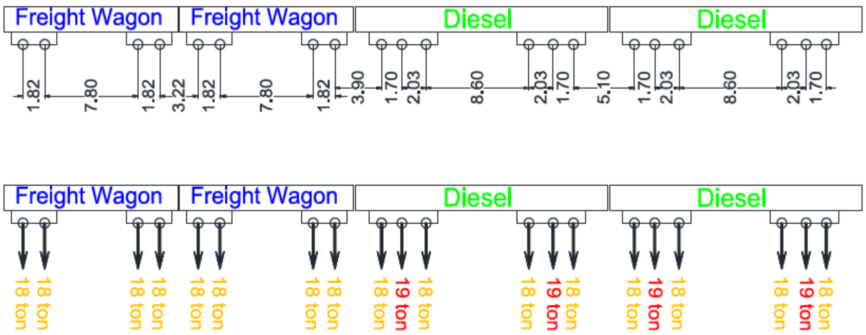

(b)

Fig. 9 (a) Test train, (b) Schematic demonstration of test train's axle loads and spacing

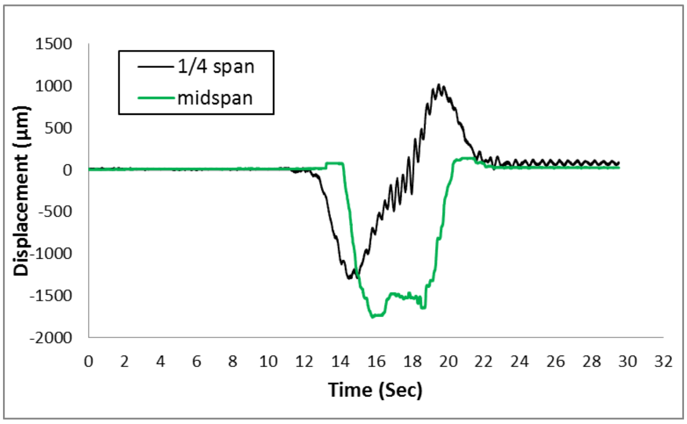

Fig. 10 Vertical Deflection of quarter and middle span, as a train passes over Veresk with a speed of 50 km/h (Veresk to Dogal)

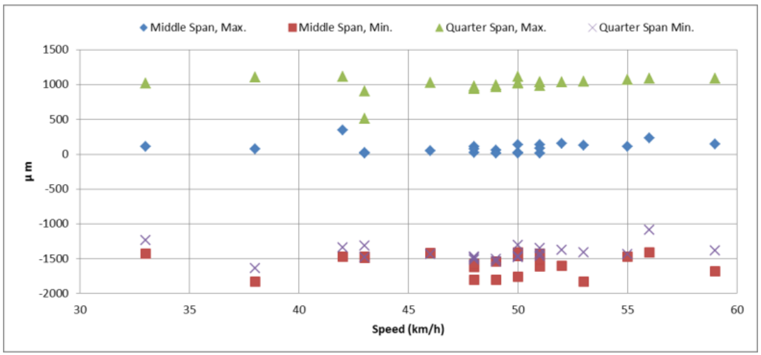

Fig. 11 Max. and Min. recorded vertical deflection of middle and quarter span of Veresk

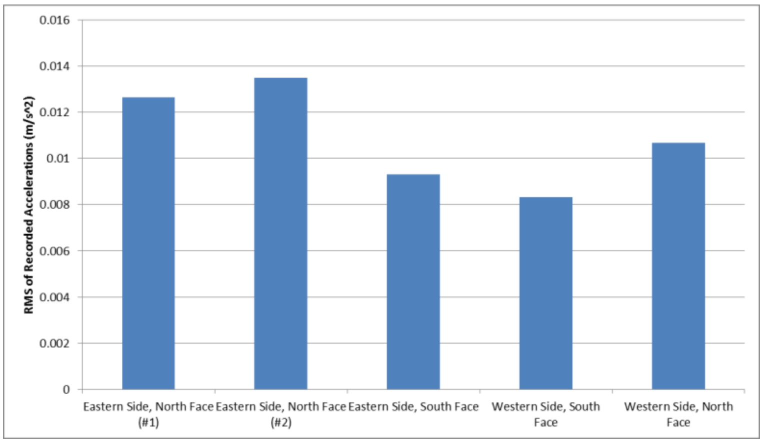

Fig. 12 RMS of recorded acceleration signature, as test train passes over Veresk with a speed of 56 km/h, from Dogal to Veresk

Fig. 11 presents the maximum and minimum recorded vertical deflections of arch's crown and quarter span for varying speeds of 30 to 60 km/h in both directions. According to Fig. 11, minimum vertical deflections of arch's crown and quarter span are almost constant for all speeds, which suggest high rigidity of the bridge. Maximum vertical deflections of middle and quarter span of Veresk are 1.8 and 1.5 mm, respectively.

In order to compare the vibration level in different spots of the bridge, root mean square of recorded acceleration signatures are calculated and presented in Figs. 12 and 13. Fig. 12 suggests that vibration levels of northern spots of the bridge are higher than those in southern spots of the bridge. This could be explained by the fact that according to as-built plans, southern part of the bridge is filled with filler concrete, while northern part has no filler concrete. According to Fig. 13, RMS of recorded acceleration signatures are directly correlated with train's crossing speed as expected.

5. Numerical model of Veresk

To study the possibility of increasing the allowable axle load of Veresk, a 3D finite element

Fig. 14 3D F.E. model of Veresk in ABAQUES

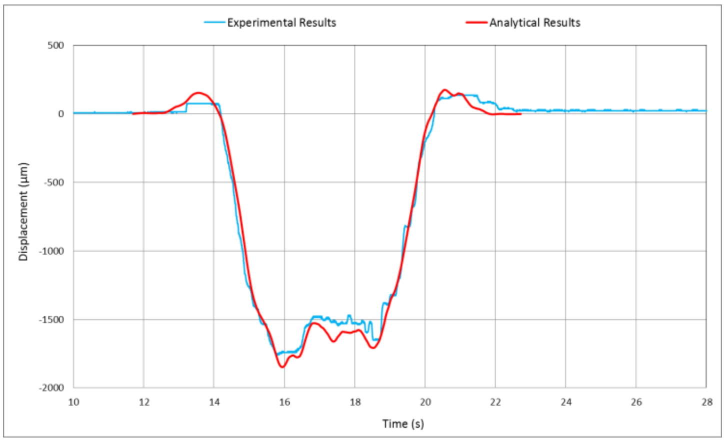

Fig. 15 Displacement signature of middle span as obtained by numerical model and field tests, for a train speed of 50 km/h (Veresk to Dogal)

model of the bridge is modeled in ABAQUES software, as shown in Fig. 14. Since Veresk rests on rock foundations, restrain points are modeled as fixed points. The model is developed by 8 points solid elements and a mesh size of 40 cm, which adds up to a total of 59905 elements and 78275 points.

The finite element model of the bridge is calibrated to minimize the differences between analytically and experimentally estimated modal properties by changing uncertain modeling parameters such as material properties and boundary conditions. Modulus of elasticity is used as a calibration parameter for the bridge, and will be modified to make sure that the numerical model conforms to the response of Veresk bridge in terms of vertical deflection, as shown in Fig. 15. According to UIC 778-3, the difference between experimental and analytical deflections shall be less than 25%, which according to Fig. 15 is satisfied.

To verify the calibrated model, two approaches are taken. First, analytical and experimental mid-span deflections for other test runs are compared, as presented in Fig. 16. As the second approach, analytical and experimental natural frequencies are compared. Table 2 presents the analytical and experimental natural frequencies of the bridge. Free vibration segments of acceleration signatures are considered in calculating the natural frequencies of field test results by

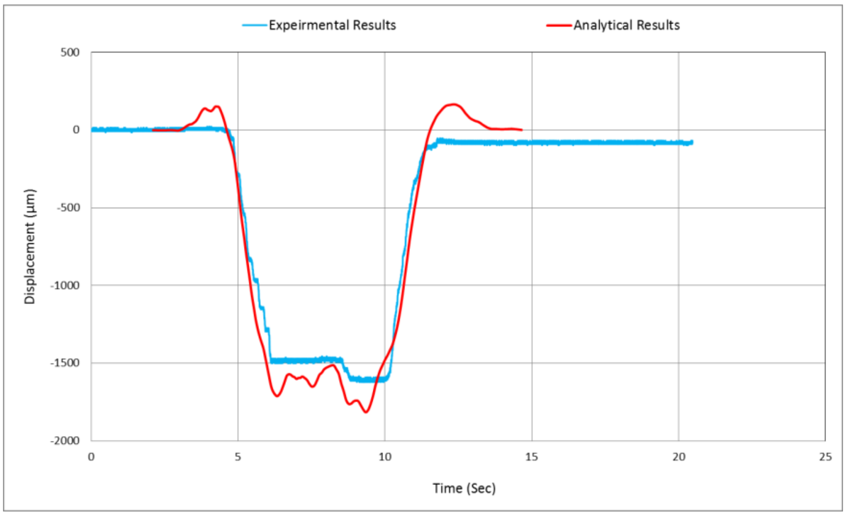

Fig. 16 Displacement signature of middle span as obtained by numerical model and field tests, for a train speed of 48 km/h (Dogal to Veresk)

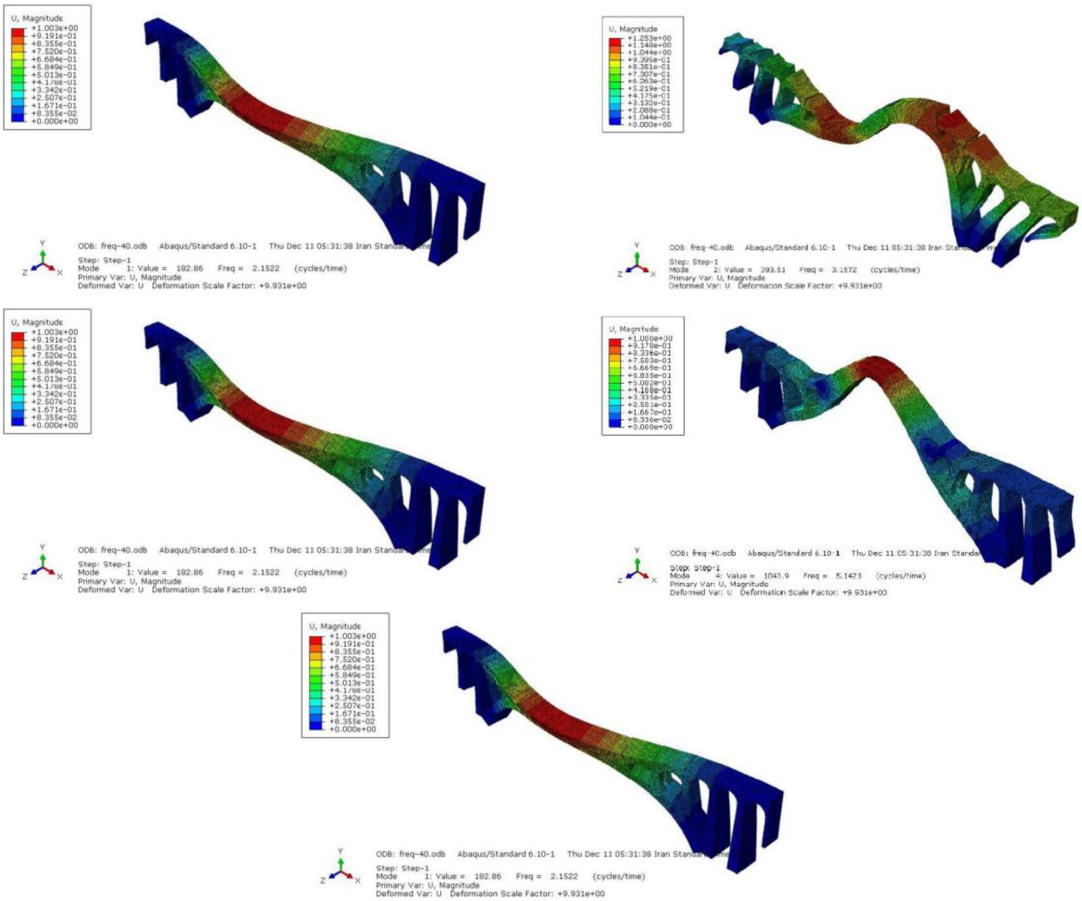

Fig. 17 Mode shapes of Veresk derived from numerical model in ABAQUES

Table 2 Experimental and analytical natural frequencies of Veresk (Hz)

Mode Shape #	1st	2nd	3rd	4th	5th
Analytical	2.2	3.2	4.1	5.1	5.8
Experimental	2.3	3.0	4.1	5.3	5.6

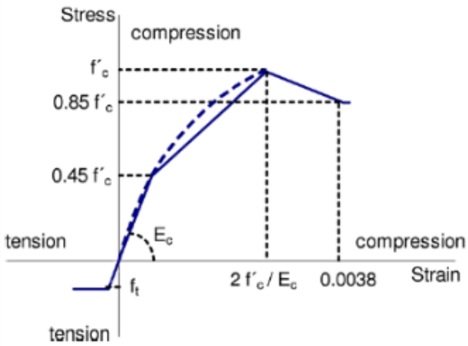

Fig. 18 Stress-strain diagram for concrete material

pick picking method. According to UIC 778-3, the difference of measured and calculated frequencies of 1st and 2nd modes shall not have a significant difference (15% for the first mode, and 25% for the second mode). According to Table 2, the difference of measured and calculated natural frequencies of first five mode shapes are less than 10%. Fig. 17 presents five modal shapes of the bridge, which are determined by analytical model.

5.1 Assessing adequacy factor of Veresk

4-hinge mechanism is the most probable mode of failure in single-ring arches (Audenaert *et al*. 2007). Hence, numerical model is employed to determine the critical train load that leads to a 4-hinge mechanism and failure of Veresk. Non-linear modeling of concrete is employed, which allows for non-linear model assessment and occurrence of plastic hinges in the model. Concrete damage plasticity model is used as the constitutive model of concrete material of the bridge. Fig. 18 shows the stress-strain diagram of concrete material (Park and Pauly 1975). In Fig. 18, E_c and f'_c are concrete's elasticity modules and compressive strength, respectively. Concrete strength due to tension is considered to be f_t which is equal to 0.63 $f'^{0.5}_c$ (MPa) (ACI 318-02).

To determine the critical position of train on the bridge, train loading is applied in middle and quarter of the span. Results suggested that applying the load in the middle of the span is more critical in terms of induced stresses on the bridge. Fig. 20 shows the developed plastic hinges due to applying UIC 776-1 loading scheme (Fig. 21) in the middle of span. Load-deformation curve is also presented in Fig. 19, in which the vertical axis is the axle load of the train, and the horizontal axis is the vertical deflection of span's keystone. The axle load corresponding to the occurrence of 4-hinge mechanism is 89.3 tons. By considering an axle load of 25 tons, adequacy factor of Veresk could be determined by Eq. (3) as follows

$$A.F. = \frac{Critical\ Axle\ Load}{Permissible\ Axle\ Load} = \frac{89.3}{25} = 3.57 \quad (3)$$

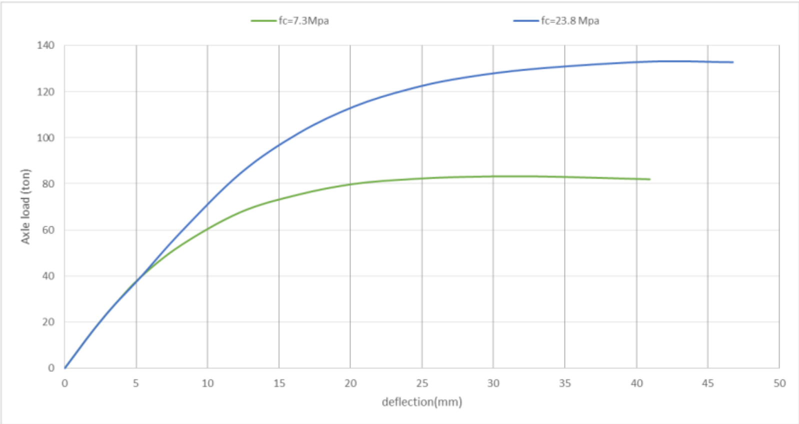

Fig. 19 Load-deflection curve

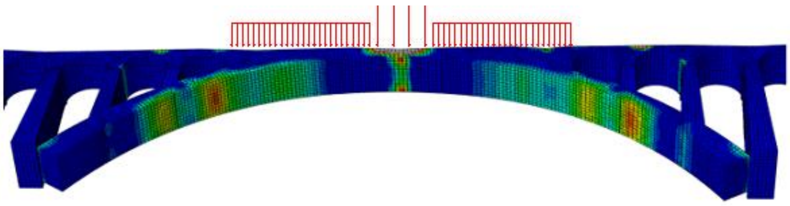

Fig. 20 Occurence of 4-hinge mechanism due to the application of train load in the middle of main span in numerical model of Veresk

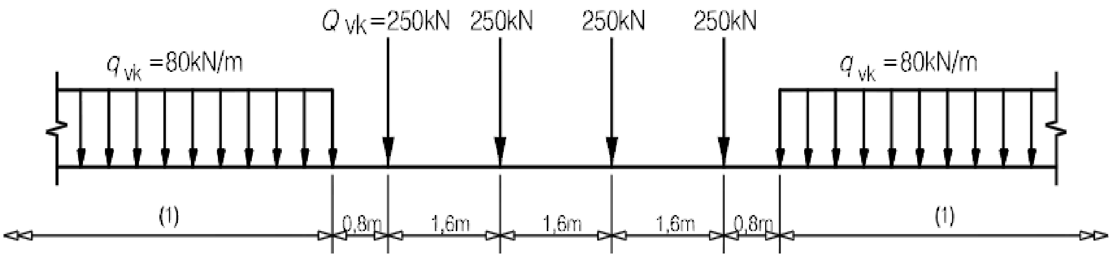

Fig. 21 Train formation adopted from UIC776-1 (2011)

Masonry compressive strength of UIC778-3 is proposed for stone masonry, while Veresk is made of concrete masonry. In this respect, compressive strength of masonry is calculated based on the method of Fortes *et al*. (2015), which is proposed for concrete masonry. They have studied the relationship between the compressive strength of ungrouted and grouted masonry and the compressive strength of the masonry unit by conducting a comprehensive test program. Using statistical methods, they have presented a set of equations to determine the compressive strength of masonry. Using the proposed equations by Fortes *et al.* masonry efficiency and compressive strength are 0.85 and 23.8 MPa, respectively. Considering a compressive strength of 23.8 MPa for masonry, corresponding axle load causing 4-hinge mechanism is 132.5 tons, and Veresk adequacy factor is 5.3, which is 33% more than that determined by considering the UIC 778-3 compressive strength of masonry.

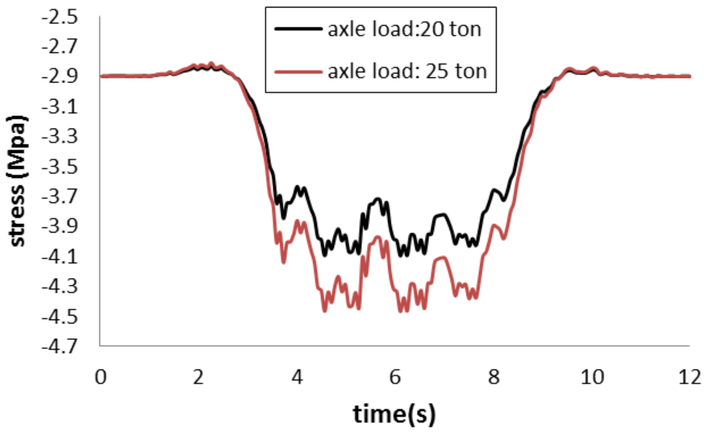

Fig. 22 Time history of compressive strain on the top fiber of Veresk's key stone, due to UIC776-1 loading scheme with axle loads of 20 and 25 tons

5.2 Fatigue capacity of Veresk

An important factor in health monitoring of old bridges is assessing the fatigue life expectancy of the bridge. Currently it is assumed that the safe capacity for masonry is around 50% of the ultimate limit state. However, allowing the bridge to be used at 50% of its ultimate capacity may induce stresses that would result in premature failure. According to equations presented in (S.B 4.7 2007), number of cycle leading to failure for a single-ring arch due to compression fatigue is determined by Eq. (4)

$$S = A \times N^{-B(1-R)} \tag{4}$$

In which:

S= the ratio of maximum stress to compressive strength for any train scheme,

N= Number of train passages leading to failure,

R= the ratio between minimum and maximum stress in each cycle,

A and B= constants which depend on the level of confidence.

Fig. 22 demonstrates the compressive stress signature of top fiber of Veresk's key stone. According to Fig. 22, minimum compressive stress due to the combination of dead and permanent loads is 2.9 MPa. Maximum compressive stresses for axle loads of 20 and 25 tons due to the combination of dead and permanent loads are 4.10 and 4.47, respectively. Considering a compressive strength of 7.3 (as derived by Eq. (2)), employing Eq. (4) and considering a confidence level of 0.95, number of cycles leading to failure are 1.4E10 and 2.42E7 for axle loads of 20 and 25 tons, respectively. Taking the compressive strength of masonry based on proposed method of Fortes *et al.* (2015) in to consideration, the value of 'S' is less than 0.5 and no fatigue failure will occur.

6. Conclusions

Results of field tests carried out on Veresk are presented in this paper. Having the bridge instrumented with deflection meters and accelerometers, the response of Veresk to different loading schemes is recorded. To assess the adequacy factor and fatigue life of the bridge, a 3D finite element model of Veresk is developed, which is calibrated using the results of field tests. By considering the 4-hinge mechanism as the failure mechanism of Veresk, an adequacy factor of 3.57 for an axle load of 25 tons is determined. Results of dynamic analysis are used to determine the fatigue life of Veresk. Results suggest that the number of cycles leading to failure will decrease by 0.2%, if axle load increases from 20 tons to 25 tons.

Acknowledgments

The authors would like to thank the financial support of Iranian railway organization, under project number 31/84235 with industrial cooperation office of Iran University of science and technology.

References

ACI 318-02 (2002), "Building Code Requirements for Structural Concrete", American Concrete Institute, Detroit, MI.

Ataei, S., Jahangiri, M. and Kazemi, V. (2016), "Evaluation of axle load increasing on a monumental masonry arch bridge based on field load testing", *J. Constr. Build. Mater.*, **116**, 413-421.

Audenaert, A., Peremans, H. and Reniers, G. (2007), "An analytical model to determine the ultimate load on masonry arch bridges", *J. Eng. Math.*, **59**, 323-336.

Bayraktar, A., Altunisik, A., Birinci, F., Sevim, B. and Turker, T. (2010), "Finite-element analysis and vibration testing of a two-span masonry arch bridge", *ASCE J. Perform. Constr. Facil.*, **24**, 46-52.

Brencich, A. and Sabia, D. (2007), "Experimental identification of a multi-span masonry bridge: the Tanaro bridge", *J. Constr. Build. Mater.*, **22**, 2087-2099.

Caglayan, B.O., Ozakgul, K. and Tezer, O. (2012), "Assessment of a concrete arch bridge using static and dynamic load test", *Struct. Eng. Mech.*, **41**(1), 83-94.

Cancelliere, I., Imbimbo, M. and Sacco, E. (2010), "Experimental tests and numerical modeling of reinforced masonry arches", *J. Eng. Struct.*, **32**, 776-792.

Casas, J.R. (2009), "A probabilistic fatigue strength model for brick masonry under compression", *J. Constr. Build. Mater.*, **23**, 2964-2972.

Chandra, J.M., Ramaswamy, A. and Manohar, C.S. (2013), "Safety assessment of a masonry arch bridge: filed testing and simulations", *ASCE J. Bridge Eng.*, **18**, 162-171.

Clemente, P., Occhiuzzi, A. and Railthel, A. (1995), "Limit behavior of stone arch bridges", *ASCE J. Struct. Eng.*, **121**(7), 1045-50.

de Felice, G. (2009), "Assessment of the load-carrying capacity of multi-span masonry arch bridges using fiber beam elements", *J. Eng. Struct.*, **31**, 1634-47.

Department of Transport (1997), "Design manual for roads and bridges", **3**, Sec. 4, Part 4, The Assessment of highway bridges and structures, London, UK.

Fortes, E., Parsekian, G. and Fonseca, F. (2015), "Relationship between the compressive strength of concrete masonry and the compressive strength of concrete masonry units", *J. Mater. Civil Eng.*, **27**(9), 04014238.

Havey, W. (1988), "Application of the mechanism analysis to masonry arches", *ASCE J. Struct. Eng.*, **66**(5), 77-84.

Helmerich, R., Niederleithinger, E., Trela, C., Bien, J., Kaminski, T. and Bernardini, G. (2010), "Multi-tool inspection and numerical analysis of an old masonry arch bridge", *J. Struct. Infrastr.*, **8**, 27-39.

Marefat, M., Ghahremani, E. and Ataei, S. (2004), “Load test of a plain concrete arch railway bridge of 20-m span”, *J. Constr. Build. Mater.*, **18**, 661-667.

Melbourne, C., Tomor, A.K. and Wang, J. (2004), “Cyclic load capacity and endurance limit of multi-ring Masonry arches”, *ARCH04 Conference*, Barcelona, Spain, November.

Newhook, J.P. and Edalatmanesh, R. (2013), “Integrating reliability and structural health monitoring in the fatigue assessment of concrete bridge decks”, *J. Struct. Infrastr. Eng.*, **9**, 619-633.

Oliveira, D., Lourenco, P. and Lemos, C. (2010), “Geometric issues and ultimate load capacity of masonry arch bridges from the northwest Iberian peninsula”, *J. Eng. Struct.*, **32**, 3955-3965.

Park, R. and Pauly, T. (1975), *Reinfoced Concrete Structures*, John Wiley and Sons.

Prentice, D.J. and Ponniah, D. (1994), “Testing of multi-span model of masonry arch bridges”, *Proceeding Centenary Year Bridge Conference*, Cardiff, England.

SB 4.7. (2007), “Structural assessment of masonry arch bridges”, Prepared by Sustainable bridges.net.

UIC 776-1 (2006), *Loads to be Considered in Railway Bridge Design*, 5th Edition.

UIC 778-3 (2011), *Recommendations for the Inspection, Assessment and Maintenance of Masonry Arch Bridges*, 2nd Edition.

CC